A R C H I V E S O F M E T A L L U R G Y A N D M A T E R I A L S
Volume 55 2010 Issue 2

T. CZUJKO*,***, R.A. VARIN**, Z. ZARAŃSKI***, Z. S. WROŃSKI*

THE DEHYDROGENATION PROCESS OF DESTABILIZED $NaBH_4$-MgH_2 SOLID STATE HYDRIDE COMPOSITES

PROCES WYDZIELANIA WODORU Z DESTABILIZOWANYCH KOMPOZYTÓW NA BAZIE WODORKÓW STAŁYCH $NaBH_4$-MgH_2

The composite behaviour of sodium borohydride – magnesium hydride mixtures was investigated. Mutual influence of both hydrides on their decomposition process was studied. The ($NaBH_4$+MgH_2) composite hydride system was synthesized in a wide range of compositions by controlled mechanical (ball) milling in a magneto-mill. In effect, nanocomposites having nanometric grain sizes of the constituent phases residing within micrometric-sized particles were produced. The dehydrogenation process of obtained composites was investigated by Differential Scanning Calorimetry (DSC) method. It is shown that the hydrogen desorption temperature of the composite constituent with the higher desorption temperature in the ($NaBH_4$+MgH_2) system substantially decreases linearly with increasing volume fraction of the constituent having lower desorption temperature which is similar behavior to well-known composite Rule-of-Mixtures (ROM) for structural composites. It is also shown that in the ($NaBH_4$+MgH_2) composite the constituents such as MgH_2 and $NaBH_4$ decompose separately and destabilization of the composite constituent with a higher desorption temperature is unrelated to the formation of MgB_2 intermetallic phase. Therefore, the improved dehydrogenation properties for $NaBH_4$ is likely due to the presence of nanostructured metallic Mg which acts as a catalyst. It is also shown that, most likely, the $NaBH_4$ constituent act as a catalyst for the accelerated decomposition of MgH_2.

Keywords: Hydrogen storage materials; Mechanical milling; Nanocomposite hydrides; Magnesium hydride; Sodium borohydride; X-ray diffraction; Lattice parameters; Nanograin size; Differential scanning calorimetry

W pracy przedstawiono wyniki badań zachowań kompozytowch mieszaniny borowodorek sodu – wodorek magnezu, gdzie ocenie poddano wzajemne oddziaływanie obu wodorków na ich proces dekompozycji.

Układ kompozytów wodorkowych ($NaBH_4$+MgH_2) syntetyzowany był w szerokim zakresie składów, poprzez kontrolowane mielenie mechaniczne (kulowe), w młynku magnetycznym. W efekcie powyższego procesu wytworzono nanokompozyty, których składniki fazowe posiadają ziarna o nanometrycznej wielkości, występujące w mikrometrycznych cząstkach. Proces odwodorowania uzyskanych kompozytów badano z wykorzystaniem metody kalorymetrycznej DSC (Differential Scanning Calorimetry). Wykazano, że temperatura desorbcji wodoru składnika kompozytu o wyższej temperaturze dekompozycji w układzie ($NaBH_4$+MgH_2) istotnie obniża się liniowo wraz ze wzrostem udziału objętościowego składnika o niższej temperaturze dekompozycji, zachowując się w sposób podobny do obowiązującej dla kompozytów strukturalnych reguły mieszanin ROM (Rule-of-Mixtures). Wykazano ponadto, iż w kompozycie ($NaBH_4$+MgH_2) jego składniki, MgH_2 i $NaBH_4$, dekomponują oddzielnie i destabilizacja składnika o wyższej temperaturze desorbcji nie jest związana z powstawaniem fazy międzymetalicznej MgB_2. Stąd też poprawa właściwości do odwodorowania $NaBH_4$ jest prawdopodobnie spowodowana obecnością nanostrukturalnego, metalicznego Mg, który działa katalitycznie. Dodatkowo wykazano, że $NaBH_4$ najprawdopodobniej działa katalitycznie na przyśpieszenie dekompozycji MgH_2.

1. Introduction

Hydrogen storage in solid state i.e. in hydrides with high hydrogen capacities is the most convenient solution for off-board storage in all transportation applications powered by Proton Exchange Membrane (PEM) fuel cell stacks. In general, solid hydrides have higher hydrogen volumetric densities than gas and liquid storage. Moreover, they do not need excessively high pressures for storage as required for gaseous hydrogen and do not suffer large thermal losses as liquid hydrogen systems do [1-5]. Unfortunately, hydrides with hydrogen capacities

* CANMETENERGY, HYDROGEN, FUEL CELLS AND TRANSPORTATION ENERGY, NATURAL RESOURCES CANADA, 1 HAANEL DR., OTTAWA, ONTARIO, CANADA K1A 1M1
** DEPARTMENT OF MECHANICAL AND MECHATRONICS ENGINEERING, UNIVERSITY OF WATERLOO, WATERLOO, ONTARIO, CANADA N2L 3G1
*** DEPARTMENT OF ADVANCED MATERIALS AND TECHNOLOGIES, MILITARY UNIVERSITY OF TECHNOLOGY, 00-908 WARSZAWA, 2 KALISKIEGO STR., POLAND

of at least 6-7 wt.% and higher are usually characterized by high temperatures of hydrogen desorption (decomposition) [6]. Obviously, high desorption temperatures are incompatible with the waste heat generated by a PEM (Proton Exchange Membrane) fuel cell (max. ~100°C).
A full decomposition of $NaBH_4$ (sodium borohydride) to $Na+B+2H_2$ should yield ~10.7 wt% of hydrogen. However, $NaBH_4$ is a thermally stable complex hydride which melts at ~500°C and decomposes close to ~570 °C [5,7]. Its standard enthalpy of formation is -188.6 kJ/molH_2 [6]. Thus, the thermal decomposition of $NaBH_4$ is irreversible and occurs in the temperature range which is beyond the practical applications for the hydrogen storage systems. Several attempts were made to destabilize $NaBH_4$ by milling it with Mg under hydrogen [8] or to directly release hydrogen from the reaction of $NaBH_4$ with chemical compounds such as $Mg(OH)_2$ [9].
It has recently been shown by Varin et al. [5,10] that by compositing high-and low-desorption temperature hydrides, the decomposition temperature of high-desorption temperature constituent obeys the rule of mixtures (ROM) similar to the one well known for engineered structural composites in the following form:

$$T_{desorption} = T^{0}_{high} - bV_{low} \tag{1}$$

where V_{low} is the volume fraction of low-desorption temperature hydride, T^{0}_{high} is the initial decomposition temperature of high-desorption temperature hydride at $V_{low}=0$ and b is the decomposition temperature difference between high and low desorption temperature hydrides: $b = T_{high} - T_{low}$. Since volume fraction (V in vol.%) is directly proportional to weight fraction (W in wt.%) Eq.(1) requires a linear dependence of decomposition temperature with a negative slope b versus either the volume or weight fraction (V_{low} or W_{low}) of a constituent hydride having lower desorption temperature.
It has already been shown that a few composite systems synthesized by ball milling which induces an intimate contact between nanostructured hydride constituents obey Eq.(1) [5,10]. One of the systems which was investigated in [5,10] is a composite between a complex hydride $NaBH_4$ having a very high temperature of decomposition and a simple metal hydride MgH_2 which has much lower decomposition temperature than $NaBH_4$ [5,6]. The present work reports the results obtained so far and explores the possible mechanisms responsible for the observed composite behavior. The composites have been synthesized in a wide range of composition by controlled mechanical milling (CMM) in a magneto-mill which in effect produced nanocomposites with the nanometric grain sizes of the constituent phases and micrometric sized particles. It is demonstrated that the hydrogen desorption in the $(NaBH_4+MgH_2)$ composite involves two steps: first, at lower temperature MgH_2 decomposes to Mg and H_2 and in a subsequent step, most likely, Mg catalyses the decomposition of $NaBH_4$. The catalytic element introduced into the system from decomposing a simple metal hydride, even with a high content of H_2, does not reduce dramatically the total capacity of the composite system. In particular, this work shows clearly that the formation of MgB_2 intermetallic phase during decomposition of both hydride constituents is not responsible for the thermodynamic destabilization of $NaBH_4$.

2. Experimental

As-received commercial MgH_2 powder (sold under the trade name MG-5026® from ABCR GmbH&Co.KG; ~98wt.% purity; the remaining Mg) and $NaBH_4$ (98% purity) from Alfa Aesar were mixed to $(NaBH_4+X\text{vol.\%}MgH_2)$ compositions where X=8, 16, 46, 63, 75 and 87 (as converted from the usual wt.%). As a reference, $NaBH_4$ and MgH_2 powders without additives were also tested. Controlled Mechanical Milling (CMM) was carried out for 5 and 20h in the hydrogen gas atmosphere under 600 kPa pressure in the magneto-mill Uni-Ball-Mill 5 manufactured by A.O.C. Scientific Engineering Pty Ltd, Australia [5, 11-13] using a strong shearing mode (HES57-two magnets) mode (Fig.1). The distance between NdFeB external magnet and milling vial (working distance–WD) was 10 and 2 mm, the ball-to-powder weight ratio was ~40 and the rotational speed of milling vial was ~175 rpm.

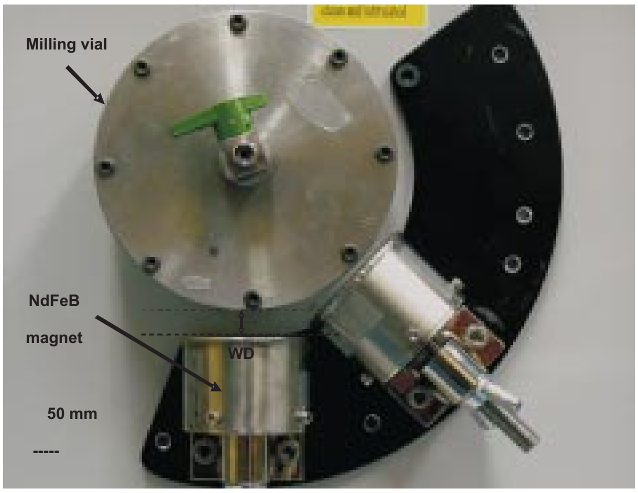

Fig. 1. Angular positions of Nd-Fe-B super-strong magnets for ball milling under high energy impact mode in the Uni-Ball-Mill

To explain the role of Mg which is formed during the decomposition process of magnesium hydride constituent in a composite, the composites of sodium borohydride with the content of metallic Mg the same as the content of MgH_2 for a few selected compositions were milled under the same conditions as the ($NaBH_4$+MgH_2) composites. To avoid hydrogenation of magnesium during milling, hydrogen in a milling vial was replaced by an argon protective gas. The details of milling process and chemical composition of various mixtures are presented in Table 1. After loading with the as received powder, an air-tight milling vial having an O-ring and equipped with a pressure valve mounted in the lid, was always evacuated and purged several times with high purity argon (Ar) gas before final pressurization with H_2 or Ar to ~600 kPa. All the powder handlings after milling were performed in a purged glove box under high purity argon.

TABLE 1

The compositions and parameters of milling process

Composite	Gas/Press. [kPa]	$R_{B/P}$	WD [mm]	Mode	Milling time [h]
$NaBH_4$	H/600	40	10/2	HES57	5
$NaBH_4$ + 8vol.% MgH_2	H/600	40	10/2	HES57	5
$NaBH_4$ + 16vol.% MgH_2	H/600	40	10/2	HES57	5
$NaBH_4$ + 43vol.% MgH_2	H/600	40	10/2	HES57	5
$NaBH_4$ + 16vol.% MgH_2	H/600	40	10/2	HES57	20
$NaBH_4$ + 43vol.% MgH_2	H/600	40	10/2	HES57	20
$NaBH_4$ + 63vol.% MgH_2	H/600	40	10/2	HES57	20
$NaBH_4$ + 75vol.% MgH_2	H/610	40	10/2	HES57	20
$NaBH_4$ + 87vol.% MgH_2	H/600	40	10/2	HES57	20
$NaBH_4$ + 30vol.% MgH_2	H/600	40	10/2	HES57	20
$NaBH_4$ + 8vol.% MgH_2	H/600	123	10/2	HES57	0.25*
$NaBH_4$ + 16vol.% MgH_2	H/600	123	10/2	HES57	0.25*
MgH_2	H/600	40	10/2	HES57	20
$NaBH_4$ + 8vol.%Mg**	Ar/600	40	10/2	HES57	20
$NaBH_4$ + 43vol.%Mg**	Ar/600	40	10/2	HES57	20
$NaBH_4$ + 63vol.%Mg**	Ar/600	40	10/2	HES57	20
$NaBH_4$ + 87vol.%Mg**	Ar/600	40	10/2	HES57	20

* Mixing previously milled powders (both powders were pre-milled for 20h/HES57/H_2)

** A mixture with Mg content equivalent to particular content (vol.%) of MgH_2

The crystalline structure of as milled and reference powders was characterized by Rigaku Rotaflex D/Max B rotating anode powder diffractometer. Monochromated $CuK\alpha_1$ radiation (λ=0.15406 nm) was used in this study produced at an accelerating voltage of 50 kV and a current of 180 mA. The scan range was from 2θ = 10 to 90° and the scan rate was 1.2°min^{-1} at the step size of 0.02°. The nanograin (crystallite) size of phases residing in the milled powders was calculated from the broadening of their respective XRD peaks using software of the system. Morphological examination of powders was conducted with high-resolution, field emission SEM (FE SEM) LEO 1530 equipped with integrated EDAX Pegasus 1200 EDS/OIM. The size measurement of the powder particles for various samples was carried out by attaching loose powder to the sticky carbon tape and taking pictures under SE mode in SEM. The images were analyzed by the Image Tool v.3.00 software. The size of the powders was calculated as the particle Equivalent Circle Diameter,

$$ECD = \sqrt{\frac{4 \cdot A}{\pi}}, \tag{2}$$

where A represents the projected particle area.

The thermal behavior of powders was studied by differential scanning calorimetry (DSC) (SETARAM Labsys™ and Netzsch 404) of ~10 mg powder sample with heating rate of 10°C/min and argon flow rate of 50 ml/min.

3. Results and discussion

3.1. Morphology and phase composition of nanocomposites

Fig.2 shows SEM micrographs of the as received powder of $NaBH_4$ and MgH_2 as well as the powders of milled ($NaBH_4$+MgH_2) nanocomposites with a low content of magnesium hydride (8÷46 vol.%). The particles of as received sodium borohydride and magnesium hydride powders (Fig. 2a, b) have irregular shapes and average size around 145 µm and 36 µm, respectively. After milling, the particle size of MgH_2 seems to be slightly refined and the particles are uniformly distributed in a volume of $NaBH_4$ particles.

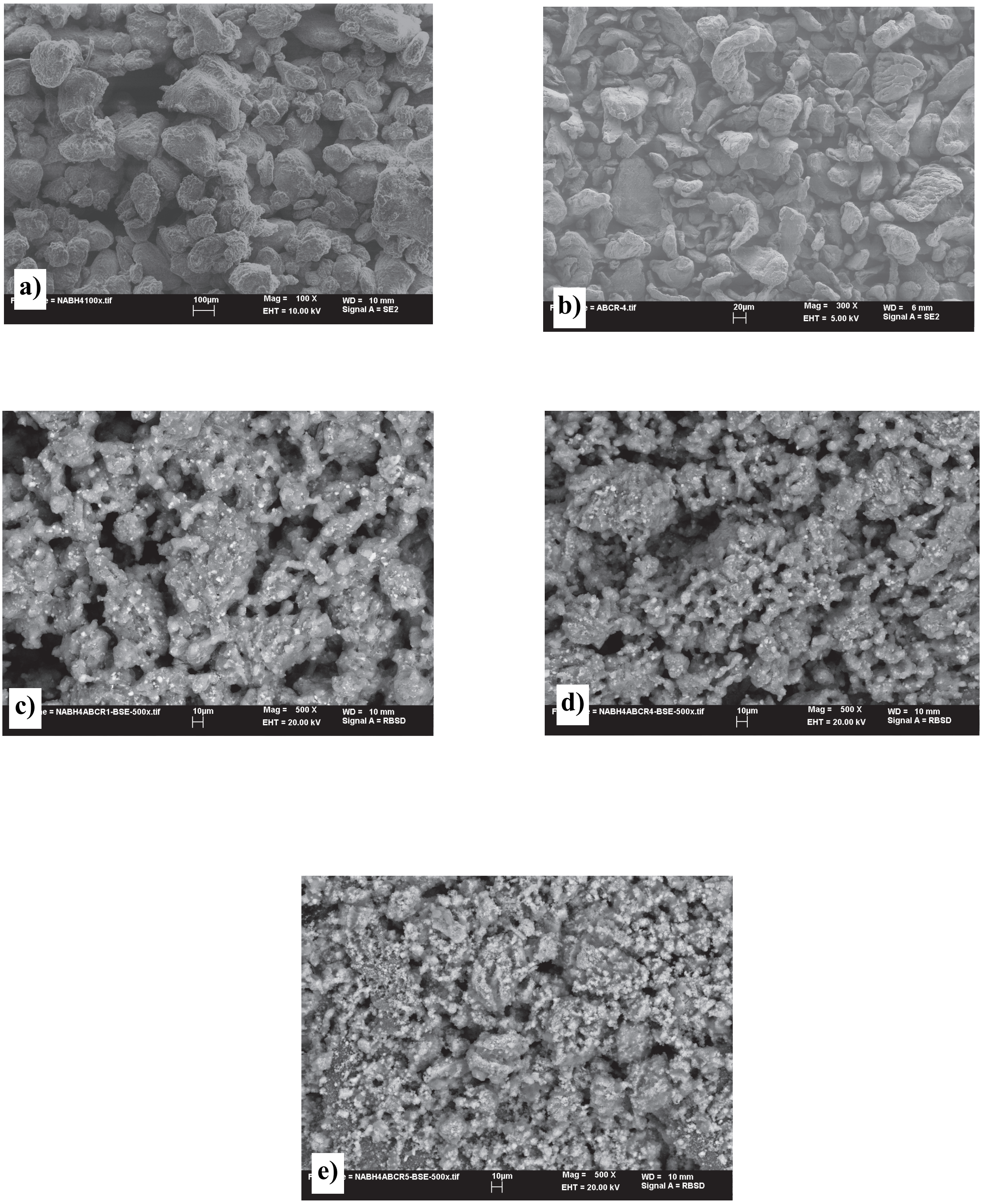

Fig. 2. SEM micrographs of the as received powder of (a) $NaBH_4$ and (b) MgH_2, and the composite powders after ball milling for (c) $NaBH_4$+8vol.% MgH_2, (d) $NaBH_4$+16vol.% MgH_2 and (e) $NaBH_4$+43vol.% MgH_2

The composites having higher contents of MgH_2 (Fig.3) show visible particle size reduction (~ 40 times). It is clearly seen that milling conditions are strongly dependent on composite composition. The efficiency of milling process (MgH_2 particle size reduction) is much higher for composites with magnesium hydride content higher than 43 vol.%.

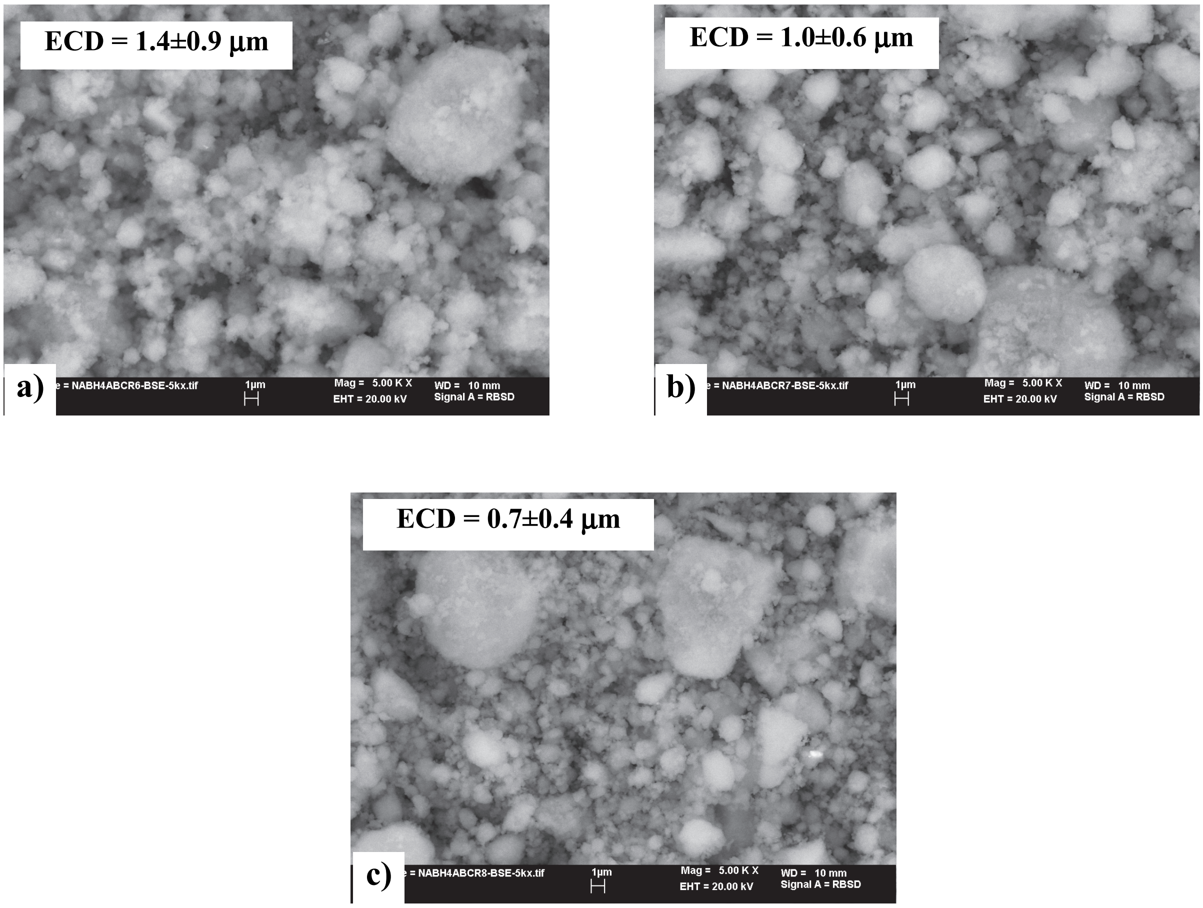

Fig. 3. SEM micrographs of composite powders after ball milling for (a) $NaBH_4$+63 vol.% MgH_2, (b) $NaBH_4$+75 vol.% MgH_2 and (c) $NaBH_4$ + 87 vol.% MgH_2

Quite opposite situation is observed for the ($NaBH_4$+Mg) composites. The particle size reduction of ductile magnesium is much more visible for powders with low or medium content of Mg (8÷63 vol.%). The morphology of these powders is characterized by the presence of a population of very small particles and clusters formed with these particles (Fig.4b,c,d). In a case of composite with the highest content of magnesium (87 vol.%) (Fig.4e) the Mg particles (ECD=9.2 µm) are practically identical to the as-received powder particles (Fig.4a; ECD = 9.5 µm).

Fig. 2. SEM micrographs of the as received powder of (a) $NaBH_4$ and (b) MgH_2, and the composite powders after ball milling for (c) $NaBH_4$+8vol.% MgH_2, (d) $NaBH_4$+16vol.% MgH_2 and (e) $NaBH_4$+43vol.% MgH_2

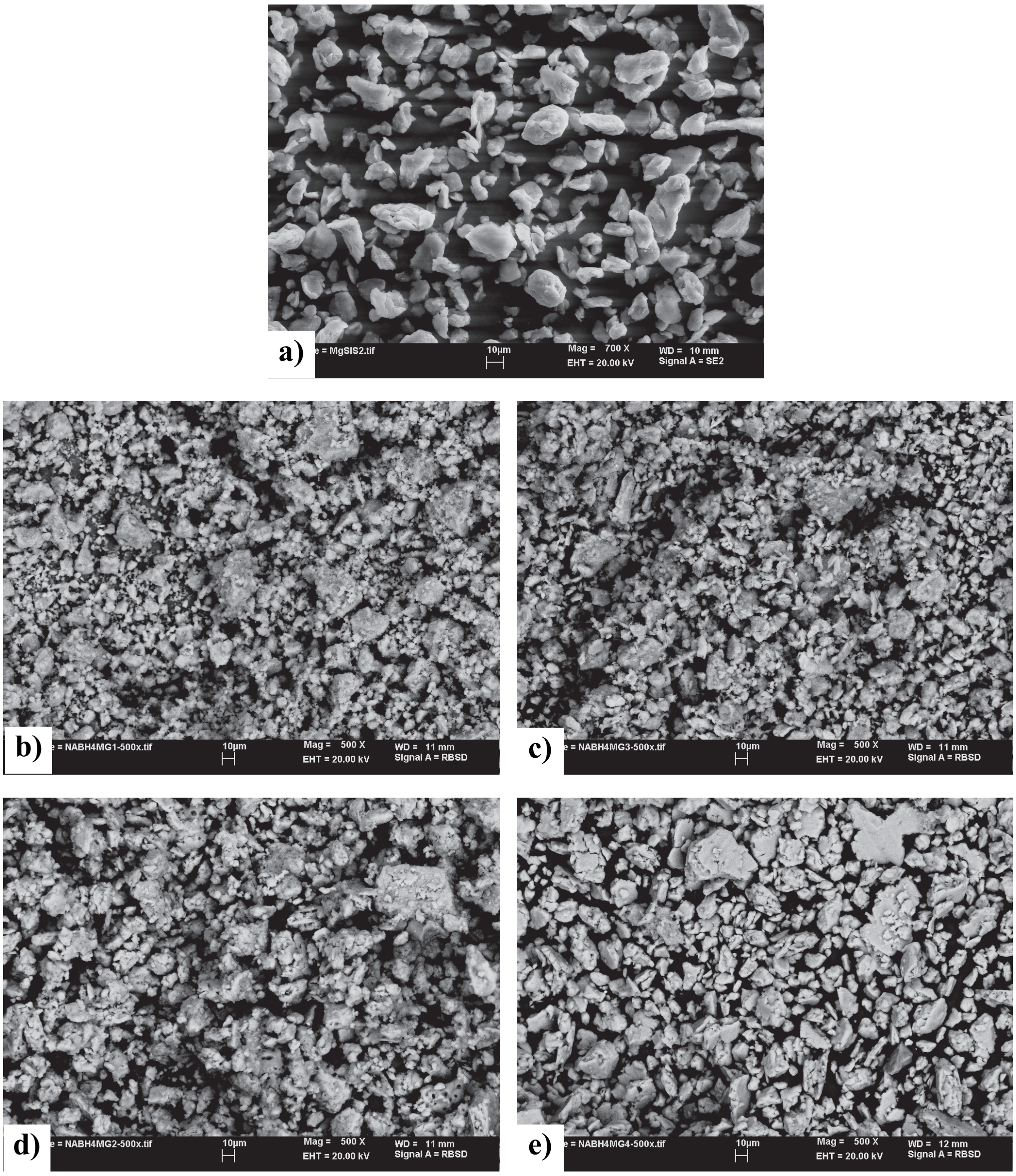

Fig. 4. SEM micrographs of (a) as received Mg powder and the composite powders after ball milling for (b) $NaBH_4$ + 8 vol.% Mg, (c) $NaBH_4$+43 vol.% Mg, (d) $NaBH_4$+63 vol.% Mg, (e) $NaBH_4$+87 vol.% Mg

Figure 5 shows the XRD patterns for the ($NaBH_4$+MgH_2) composites with a varying content of magnesium hydride. The intensity of particular peaks is related to chemical composition, but it must be pointed out that the γ-MgH_2 phase, typical for magnesium hydride after milling, appears only when the level of MgH_2 is 43 vol.%. This verifies SEM observations, that milling process starts to be effective only for composites having high content of MgH_2. This behavior is also visible from the analysis of grain size as a function of composition in Fig.6. The grain size of both constituents, NaBH4 and MgH_2, is greatly reduced for composites with the MgH_2 contents around 43 vol.% and more. It also must be noticed that nanostructuring of $NaBH_4$ is not so effective as that of magnesium hydride (Table 2). Sodium borohydride seems to act as a sort of a greasy material in a composite. It must be also noticed that increasing milling time from 5 to 20 h does not change the phase composition and grains size of analyzed composite constituents (Table 2 – $NaBH_4$+16vol.%MgH_2 and $NaBH_4$+43vol.%MgH_2).

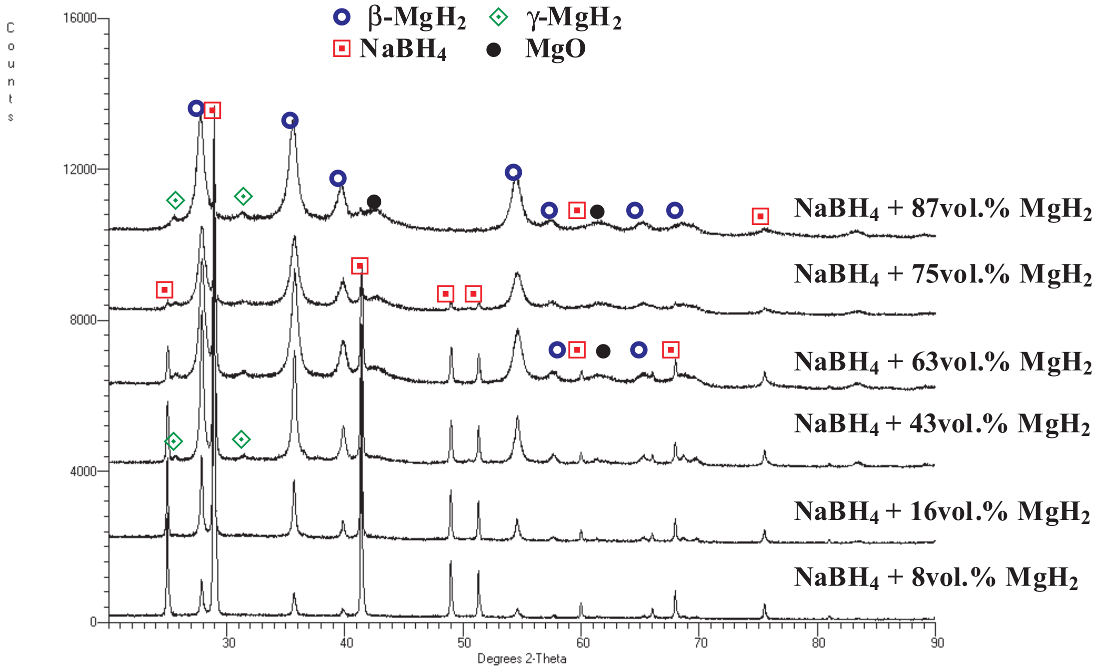

Fig. 5. XRD patterns of the ($NaBH_4$ + MgH_2) composites

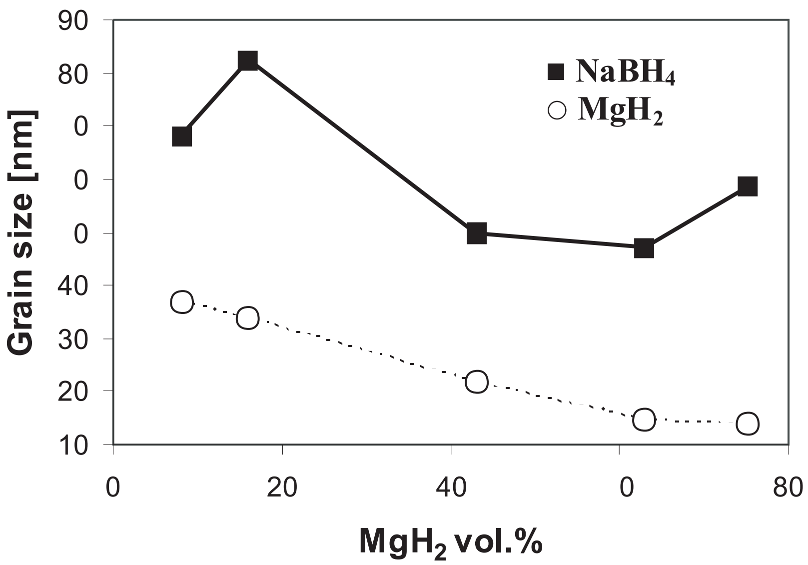

Fig. 6. Grain size of $NaBH_4$ and MgH_2 after ball milling as a function of MgH_2 content in the ($NaBH_4$+MgH_2) composites

TABLE 2

The phase composition and the grain size of Mg, MgH_2 and $NaBH_4$ in various powders

Composite	Grain size of MgH_2 [nm]	Grain size of $NaBH_4$ [nm]	Grain size of Mg [nm]	Phases present in the powder
As-received $NaBH_4$	—	77.0±15.0	—	$NaBH_4$
$NaBH_4$/milled 5h	—	85.3±3.2	—	$NaBH_4$
MgH_2/20h	12±1	—	—	MgH_2
8 vol.%MgH_2/5h	36.9±1.7	68.2±4.1	—	$NaBH_4$, β-MgH_2
16 vol.% MgH_2/ 5h	32.5±2.6	67.5±3.2	—	$NaBH_4$, β-MgH_2
43 vol.% MgH_2/5h	22.7±1.7	63.4±7.2	—	$NaBH_4$, β and γ-MgH_2, Mg, MgO
16 vol.% MgH_2/20h	34.0±3.9	82.2±7.7		$NaBH_4$, β-MgH_2
43 vol.% MgH_2/20h	21.8±1.9	49.8±1.7	—	$NaBH_4$, β and γ-MgH_2, MgO, M
63 vol.% MgH_2/20h	14.8±0.9	47.0±3.6	—	$NaBH_4$, β and γ-MgH_2, MgO
75 vol.% MgH_2/20h	14.0±1.4	58.5±12.4	—	$NaBH_4$, β and γ-MgH_2, MgO
87 vol.% MgH_2/20h	13.2±0.9	—	—	$NaBH_4$, β and γ-MgH_2, MgO
8 vol.% Mg/20h	—	Poly	Poly	$NaBH_4$, Mg, $Mg(OH)_2$
43 vol.% Mg/20h	—	?	104	$NaBH_4$, Mg, MgH_2, MgO
63 vol.% Mg/20h	—	?	103	$NaBH_4$, Mg, MgH_2, MgO, $Mg(OH)_2$
87 vol.% Mg/20h	—	?	88	$NaBH_4$, Mg, MgH_2, MgO, $Mg(OH)_2$

A different behavior is observed for the ($NaBH_4$+Mg) composites. The XRD pattern in Fig.7 shows the presence of elemental composite constitutes and the peaks of β-MgH_2. It suggests that during ball milling $NaBH_4$ partially reacts with Mg and forms β-MgH_2. The possible reactions were proposed in [5].

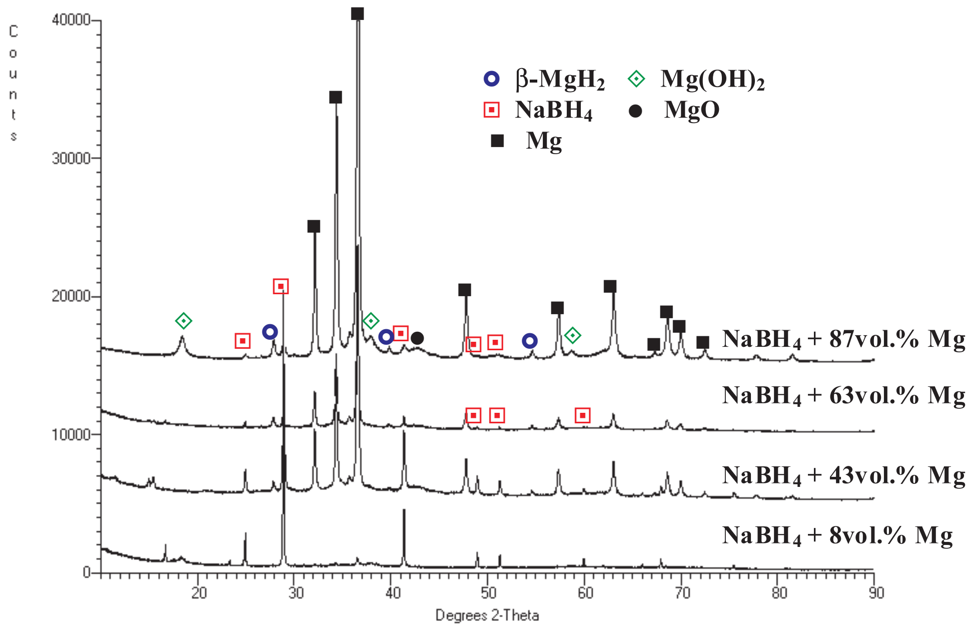

Fig. 7. XRD patterns for $NaBH_4$ composites

The grain size of as received $NaBH_4$ as well that of Mg in the composites with 8÷63vol.%Mg is close to 100 nm (Table 2). Only the composite with the highest level of 87 vol.%Mg reveals a slight grain size reduction for Mg (to 88 nm). It is clearly visible that the efficiency of milling process for sodium borohydride and magnesium hydride powders is much higher than for the powders with the magnesium additive. Peaks of $Mg(OH)_2$ in Fig. 7 for the 87 vol.%Mg composite are most likely due to the partial hydrolysis of β-MgH_2 formed during milling in a presence of hygroscopic $NaBH_4$ collecting moisture when XRD test progresses.

3.2. Thermal hydrogen desorption

Hydrogen desorption was investigated by differential scanning calorimetry (DSC) analysis. Figure 8 shows the examples of DSC curves for the investigated powders as compared to the reference DSC of the as-received commercial $NaBH_4$. The latter shows two strong, endothermic peaks with the maximum around 498.1°C and 577.2°C (Fig.8a). The first peak is related to the melting and the second to the decomposition of $NaBH_4$ in accord with result presented by Stasinevich et al. [7].

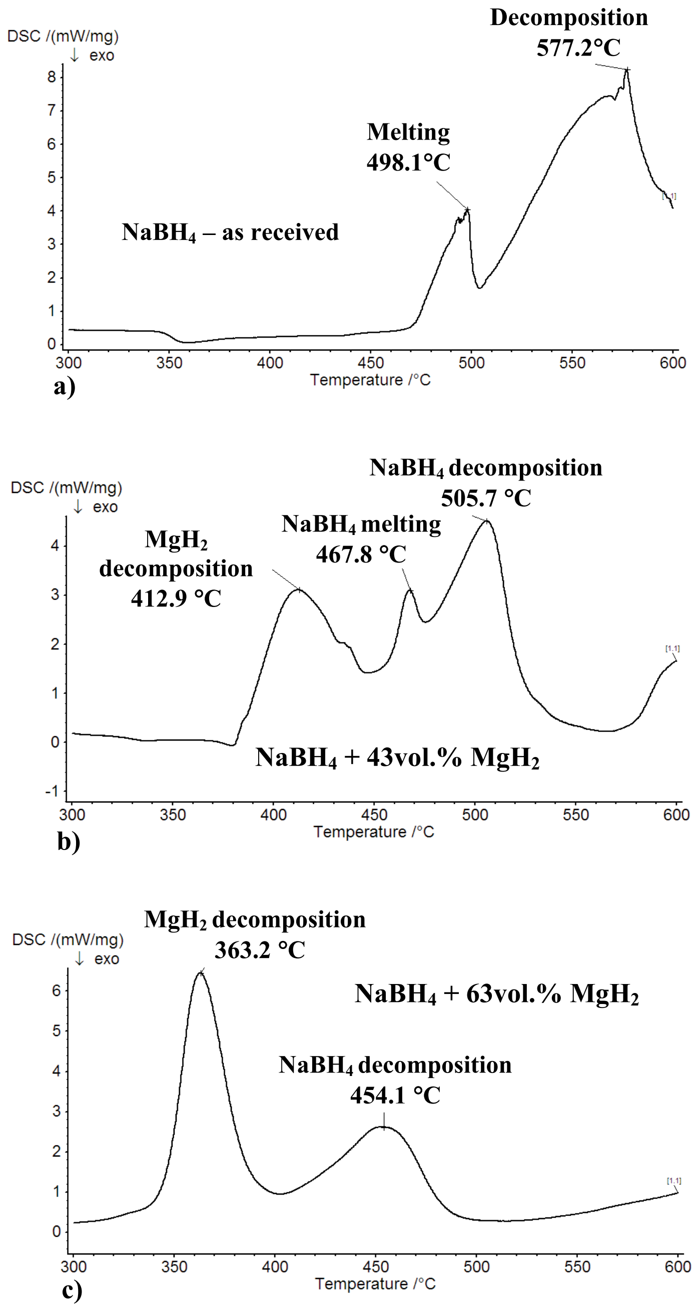

Fig. 8. DSC curves for (a) $NaBH_4$ as-received, (b) $NaBH_4$ + 46 vol.%MgH_2 and (c) $NaBH_4$ + 63vol.% MgH_2 composites

The DSC curve for the $NaBH_4$+43vol.%MgH_2 nanocomposite (Fig.8b) is characterized by three endothermic peaks. The first peak at ~413°C is related to the decomposition of MgH_2. This temperature range is comparable to the typical DSC peak of commercial MgH_2 [5,14]. The second peak at ~468°C is the melting peak of $NaBH_4$. Finally, the third peak at ~506°C is related to the decomposition of $NaBH_4$. The visible shift of peak positions for $NaBH_4$ to lower temperatures, as compared to these in Fig.8a, is clearly observed such that the decomposition peak temperature for $NaBH_4$ in this composite is quite close to the melting temperature peak for as received $NaBH_4$. Apparently, the addition of 43 vol.%MgH_2 in a visible way destabilizes $NaBH_4$ but does not change the fundamental mechanism of hydrogen desorption. The decomposition is still following the melting process. However, the situation changes dramatically for the $NaBH_4$+63vol.%MgH_2 nanocomposite (Fig.8c). The DSC curve for this nanocomposite is characterized by a single endothermic desorption peak at ~363°C from MgH_2 and a single endothermic desorption peak from $NaBH_4$ at ~454°C. It suggests that the decomposition temperature of sodium borohydride in the 63vol.%MgH_2 composite decreased below the melting point of $NaBH_4$.

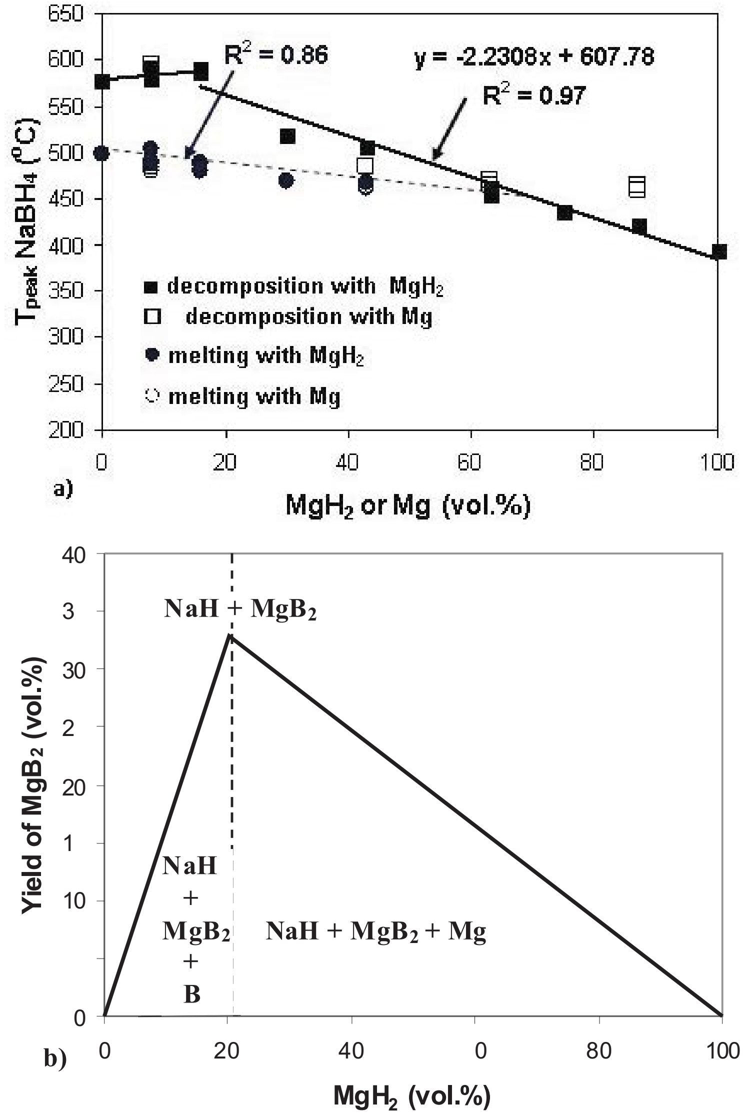

Fig. 9. The influence of MgH_2 content on the destabilization of $NaBH_4$ – (a) the $NaBH_4$ decomposition and melting DSC peak temperatures as a function of MgH_2 content; (b) The theoretical yield of MgB_2 formation for $NaBH_4$ + MgH_2 reaction as a function of MgH_2 content. Adopted from [5]

Fig.9a presents the temperatures for the melting and decomposition peaks of NaB_4 as a function of the MgH_2 or Mg content in a composite. The melting temperature of $NaBH_4$ only slightly decreases linearly with increasing content of MgH_2 or Mg. The decomposition temperature of $NaBH_4$ behaves in a more complex fashion. The MgH_2 additive in the range of 0÷20 vol.% does not change the decomposition temperature of $NaBH_4$. Increasing the amount of magnesium hydride over 20 vol.% gradually reduces the decomposition temperature of $NaBH_4$ which is eventually reduced by ~200°C for the $NaBH_4$+87vol.%MgH_2 composite. According to Vajo et al. [15-18] and Züttel et al. [19], this kind of behavior in a mixture of two hydrides could be caused by the formation of an intermetallic phase, which could change the enthalpy of the system (details see [5]). By analogy to the reaction presented by Vajo et al. [15-18] for $LiBH_4$ destabilized by MgH_2 the decomposition of the ($NaBH_4$+MgH_2) composite could proceed as follows:

$$2NaBH_4 + MgH_2 \rightarrow 2NaH + MgB_2 + 4H_2 \qquad (3)$$

It suggests that the strongest destabilization of $NaBH_4$ by MgH_2 should be observed for a composite where the yield of MgB_2 formation is the highest and that means for the stoichiometric composition ($NaBH_4$+20.5vol.%MgH_2). In Fig.9b the yield of MgB_2 formation versus composite chemical composition and theoretically predicted products of decomposition are presented. For hypo-stoichiometric compositions the composites in this range should decompose to solid products such as NaH, MgB_2 and B. Stoichiometric decomposition is characterized by the presence of only NaH and MgB_2. The hyper-stoichiometric composites decompose to NaH, MgB_2 and Mg. These theoretical phase compositions of decomposed composites are confirmed for the hyper-stoichiometric $NaBH_4$+43vol.%MgH_2 composite. To obtain a sufficient amount of powder for X-ray diffraction, the decomposition process of the above mentioned composite was conducted in a furnace rather than in a DSC apparatus, under Ar atmosphere and at temperature of 600°C. The XRD pattern of the analyzed products of decomposition is presented on Fig.10. It shows the presence of the peaks of the MgB_2 and MgO phases. It seems that the conditions of the decomposition process carried out in a furnace were insufficient to prevent the oxidation of decomposition product Mg. No Bragg peaks of NaH are observed in Fig.10. The decomposition temperature of NaH is quoted by Grochala and Edwards [6] as 425°C. If NaH indeed decomposed to metallic Na and hydrogen at the furnace temperature of 600°C then as a very low melting point metal (~100°C) it might have evaporated at such a high temperature and its Bragg peaks would not be observed in Fig.10. However, Weast et al reports 800°C [20] as its decomposition temperature so at the furnace temperature of 600°C NaH would still have been stable. The lack of NaH Bragg peaks is rather puzzling and hard to explain at the moment.

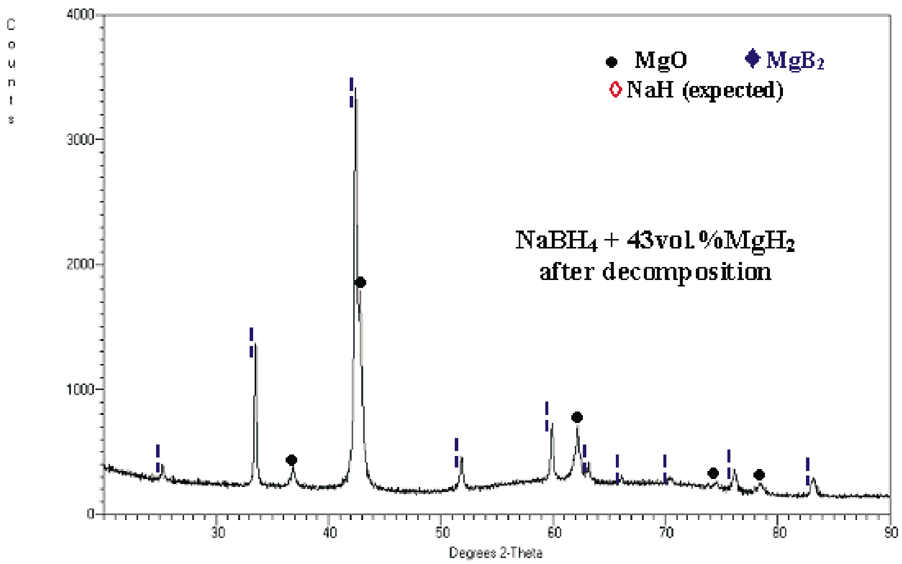

Fig. 10. XRD patterns for $NaBH_4$ + 43vol.%MgH_2 composite after decomposition at 600°C

In Fig.9a the decomposition temperature of $NaBH_4$ decreases linearly with increasing MgH_2 content only for hyper-stoichiometric composites. In contrast to the theory presented by Vajo et al. [15-18] and Züttel et al. [19] the decomposition temperature of $NaBH_4$ in the hypo-stoichiometric composites does not exhibit any increase with increasing content of MgH_2 as it would have to if their theory was correct (increase of MgB_2 content). However, it must be noticed that destabilization process described by the above authors is based on the perceived enthalpy changes. Even if $NaBH_4$ would be destabilized thermodynamically, it might have not easily decomposed due to poor kinetics. Therefore, an alternative hypothesis is that the free nanostructured Mg formed due to the decomposition of MgH_2 could act as a catalyst to increase the kinetics of decomposition of $NaBH_4$ whether or not it is destabilized thermodynamically. To confirm the catalytic effect of Mg on $NaBH_4$ we have analyzed the decomposition process of ($NaBH_4$+Mg) composites. Four composites with the contents of Mg were selected having the same vol.% as corresponding composites containing MgH_2 (Table 2). As can be seen in Fig.9a, in three out of four composites with Mg, the $NaBH_4$ constituent has a very similar decomposition temperature as $NaBH_4$ in composites with the same vol.% of MgH_2 and the data points fit well to the ROM line. Only the composite with the highest content of Mg (87 vol.%) shows a slightly higher decomposition temperature than its MgH_2 counterpart. This behavior is probably related to different mechanical properties of Mg and MgH_2 which result in different abilities to particle and grain size reduction during milling process (Fig.4 and Table 2). Most likely, for the $NaBH_4$+87 vol.%Mg composite, the intimate contact between the catalytic Mg and $NaBH_4$ complex hydride is insufficient and the catalytic effect is less pronounced in this composite.

Quite unusual behavior of the MgH_2 constituent is also observed in the ($NaBH_4$+MgH_2) composites. Fig.11 shows the DSC peak temperature for the MgH_2 constituent as a function of MgH_2 content as compared to the decomposition temperature of MgH_2 as received and milled under the same conditions as composite powders. For composites with the lower amount of MgH_2 (i.e. higher amount of $NaBH_4$) the temperature of MgH_2 decomposition is approximately the same as the decomposition temperature of as received MgH_2. Such a behavior suggests that the particle size of MgH_2 was not sufficiently reduced during ball milling, which is in accord with powder morphology observations (Fig.2 and 3). Whereas, for composites with low amount of $NaBH_4$ the decomposition temperature of MgH_2 is much lower than that for pure MgH_2 milled under the same conditions. Therefore, the question arises whether this profound DSC temperature reduction is a direct effect of ball milling and resulting reduction of nanocomposite hydride (mostly MgH_2) particle size or the catalytic effect of $NaBH_4$. Recently, we have reported that a significant refinement of the particle size (ECD) of MgH_2 to the submicrometer range 700-300 nm is responsible for a dramatic decrease of its DSC desorption temperature

[5,14,21]. However, the reduction of the desorption temperature observed in the composites with a lower $NaBH_4$ concentration is much larger than that for pure MgH_2. Therefore, it is concluded that not only the nanocomposite particle size can be responsible for the observed lowering of DSC desorption temperature of the MgH_2 constituent in the ($NaBH_4$+Xvol.%MgH_2) nanocomposites (where X= 63÷87). Normally, the milled MgH_2 having the hydride particle size of ~ 1 μm as obtained in this work (Fig.3) would be expected to have the DSC desorption peak temperature around 390-400°C as reported in [21]. Therefore, the appearance of DSC peak with the maximum at ~360°C (Fig.8c) for an intimate mixture of two dissimilar hydrides such as β-MgH_2 and $NaBH_4$ strongly suggests that both hydrides are simultaneously destabilized most likely acting catalytically on one another. We have already presented similar behavior of MgH_2 in a presence of $NaBH_4$ for the (MgH_2+$NaBH_4$) composite synthesized by reactive ball milling of Mg and $NaBH_4$ for 100h [8].

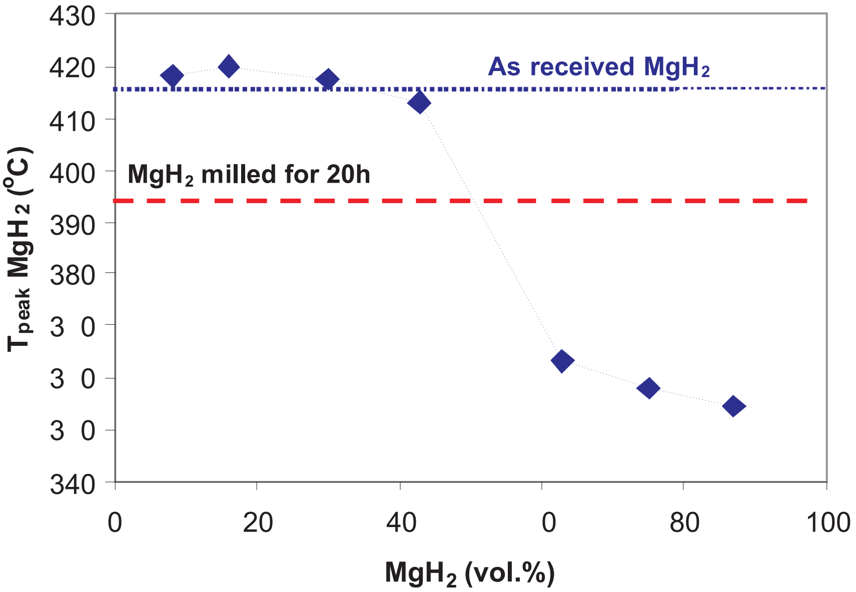

Fig. 11. The MgH_2 decomposition DSC peak temperatures as a function of MgH_2 content in the ($NaBH_4$+MgH_2) composites

4. Conclusions

The catalytic effects of MgH_2 additives on the hydrogen desorption properties of the $NaBH_4$ formed after controlled milling of the ($NaBH_4$+MgH_2) composites have been studied. The DSC desorption peak temperature of $NaBH_4$ decreases dramatically with increasing amount of MgH_2 in the composites. This effect is most likely due to the catalytic effect of Mg which is formed during MgH_2 decomposition than to thermodynamically destabilization of sodium borohydride by formation of intermediate MgB_2 intermetallic phase. Also the catalytic influence of $NaBH_4$ on MgH_2 was observed but mechanism of this behavior still needs further research.

Acknowledgements

This work was supported by a grant from the Natural Sciences and Engineering Research Council of Canada and from a grant from the State Committee for Scientific Research of Poland (N N507352735), both of which are gratefully acknowledged.

REFERENCES

[1] L. Schlapbach, A. Züttel, Hydrogen-storage materials for mobile applications. Nature **414**, 353-358 (2001).

[2] J. A. Ritter, A. D. Ebner, J. Wang, R. Zidan, Implementing a hydrogen economy. Materials Today **6(9)**, 18-23 (2003).

[3] A. Züttel, Materials for hydrogen storage. Materials Today **6(9)**, 24-33 (2003).

[4] M. Fichtner, Nanotechnological aspects in materials for hydrogen storage. Advanced .Engineering Materials **7**, 443-455 (2005).

[5] R. A. Varin, T. Czujko, Z. S. Wronski, Nanomaterials for Solid State Hydrogen Storage, Springer Science+Business Media, LLC 2009, 233 Spring Street, New York, NY 10013, USA, 2009.

[6] W. Grochala, P. P. Edwards, Thermal decomposition of the non-interstitial hydrides for the storage and production of hydrogen. Chemical Reviews. **104**, 1283-1315 (2004).

[7] D. S. Stasinevich, G. A. Egorenko, Thermographic investigation of alkali metal and magnesium tetrahydroborates at pressure up to 10 atm. Russian Journal of Inorganic Chemistry **13**, 341-343 (1968).

[8] T. Czujko, R. A. Varin, Z. S. Wronski, Z. Zaranski, T. Durejko, Synthesis and hydrogen desorption properties of nanocomposite magnesium hydride with sodium borohydride (MgH_2 + $NaBH_4$). Journal of Alloys and Compound **427**, 291-299 (2007).

[9] V. Drozd, S. Saxena, S. V. Garimella, A. Durygin, Hydrogen release from a mixture of $NaBH_4$ and $Mg(OH)_2$. International Journal of Hydrogen Energy **32**, 3370-3375 (2007).

[10] R. A. Varin, T. Czujko, Ch. Chiu, R. Pulz, Z. Wronski, Synthesis of nanocomposite hydrides for solid-state hydrogen storage by controlled mechanical milling techniques. Journal of Alloys and Compounds **483**, 252-255 (2009).

[11] A. Calka, A. P. Radlinski, Universal high performance ball-milling device and its application for mechanical alloying. Materials Science and Engineering. **A 134**, 1350-1353 (1991).

[12] Patents: WO9104810, US5383615, CA2066740, EP0494899, AU643949.

[13] A. Calka, R. A. Varin, in: Int. Symp. on Processing and Fabrication of Advanced Materials IX-PFAM IX, eds. T.S. Srivatsan, R.A. Varin, M. Khor, ASM International, Materials Park, OH, 263-287 (2001).

[14] R. A. Varin, T. Czujko, Z. Wronski, Particle size, grain size and γ -MgH_2 effects on the desorption properties of nanocrystalline commercial magnesium hydride processed by controlled mechanical milling. Nanotechnology **17**, 3856-3865 (2006).

[15] J. J. Vajo, F. Mertens, C. C. Ahn, R. C. Bowman, Jr., B. Fultz, Altering hydrogen storage properties by hydride destabilization through alloy formation: LiH and MgH_2 destabilized with Si. Journal of Physical Chemistry B **108**, 13977-13983 (2004).

[16] J. J. Vajo, S. L. Skeith, F. Mertens, Reversible storage of hydrogen in destabilized $LiBH_4$. Journal of Physical Chemistry B **109**, 3719-3722 (2005).

[17] J. J. Vajo, T. T. Salguero, A. F. Gross, S. L. Skeith, G. L. Olsen, Thermodynamic destabilization and reaction kinetics in light metal hydride systems. Journal of Alloys and Compounds **446-447**, 409-414 (2007).

[18] J. J. Vajo, G. L. Olson, Hydrogen storage in destabilized chemical systems. Scripta Materialia **56**, 829-834 (2007).

[19] A. Züttel, A. Borgschulte, S-I. Orimo, Tetrahydroborates as new hydrogen storage materials. Scripta Materialia **56**, 823-828 (2007).

[20] R. C. Weast, M. J. Astle, W. H. Beyer, CRC Handbook of Chemistry and Physics. CRC Press, Inc. 1983. Boca Raton, Florida, USA.

[21] R. A. Varin, T. Czujko, Ch. Chiu, Z. Wronski, Particle size effects on the desorption properties of nanostructured magnesium dihydride (MgH_2) synthesized by controlled reactive mechanical milling (CR-MM). Journal of Alloys and Compounds **424**, 356-364 (2006).

Received: 10 February 2010.